

Towards Diverse Perspective Learning with Selection over Multiple Temporal Poolings

Jihyeon Seong^{*1}, Jungmin Kim^{*1}, Jaesik Choi^{1,2}

¹Korea Advanced Institute of Science and Technology (KAIST), South Korea

²INEEJI, South Korea

{jihyeon.seong, aldir17, jaesik.choi}@kaist.ac.kr

Abstract

In Time Series Classification (TSC), temporal pooling methods that consider sequential information have been proposed. However, we found that each temporal pooling has a distinct mechanism, and can perform better or worse depending on time series data. We term this fixed pooling mechanism a single perspective of temporal poolings. In this paper, we propose a novel temporal pooling method with diverse perspective learning: Selection over Multiple Temporal Poolings (SoM-TP). SoM-TP dynamically selects the optimal temporal pooling among multiple methods for each data by attention. The dynamic pooling selection is motivated by the ensemble concept of Multiple Choice Learning (MCL), which selects the best among multiple outputs. The pooling selection by SoM-TP’s attention enables a non-iterative pooling ensemble within a single classifier. Additionally, we define a perspective loss and Diverse Perspective Learning Network (DPLN). The loss works as a regularizer to reflect all the pooling perspectives from DPLN. Our perspective analysis using Layer-wise Relevance Propagation (LRP) reveals the limitation of a single perspective and ultimately demonstrates diverse perspective learning of SoM-TP. We also show that SoM-TP outperforms CNN models based on other temporal poolings and state-of-the-art models in TSC with extensive UCR/UEA repositories.

Introduction

Time Series Classification (TSC) is one of the most valuable tasks in data mining, and Convolutional Neural Network (CNN) with global pooling shows revolutionary success on TSC (Långkvist, Karlsson, and Loutfi 2014; Ismail Fawaz et al. 2019). However, global pooling in TSC poses a significant challenge, as it disregards the fundamental characteristic of time series data, which is the temporal information, by compressing it into a single scalar value (Lecun et al. 1998; Yu et al. 2014). To tackle this issue, temporal pooling methods were introduced, which preserve the temporal nature of the time series at the pooling level (Lee, Lee, and Yu 2021).

Temporal pooling involves employing operations such as ‘maximum’ (MAX) and ‘average’ (AVG), categorized by segmentation types: ‘no segment,’ ‘uniform,’ and ‘dynamic.’ These segmentation types correspond respectively to

Global-Temporal-Pooling (GTP), Static-Temporal-Pooling (STP), and Dynamic-Temporal-Pooling (DTP) (Lee, Lee, and Yu 2021). We refer to each distinct pooling mechanism as a *perspective* based on the segmentation types. However, we discovered that the most effective temporal pooling varies depending on the characteristics of the time series data, and there is no universally dominant pooling method for all datasets (Esling and Agon 2012). This underlines the necessity for a learnable pooling approach adaptable to each data sample’s characteristics.

In this paper, we propose Selection over Multiple Temporal Poolings (SoM-TP). SoM-TP is a learnable ensemble pooling method that dynamically selects heterogeneous temporal poolings through an attention mechanism (Vaswani et al. 2017). Aligned with our observation that a more suitable pooling exists for each data sample, a simple ensemble weakens the specified representation power (Lee et al. 2017). Therefore, SoM-TP applies advanced ensemble learning, motivated by Multiple Choice Learning (MCL), that selects the best among the multiple pooling outputs (Guzmán-rivera, Batra, and Kohli 2012).

MCL is a selection ensemble that generates M predictions from multiple instances, computes the oracle loss for the most accurate prediction, and optimizes only the best classifier. Capitalizing on the advantage of deep networks having access to intermediate features, SoM-TP ensembles diverse pooling features in a single classifier. To achieve non-iterative optimization, SoM-TP dynamically selects the most suitable pooling method for each data sample through attention, which is optimized by *Diverse Perspective Learning Network (DPLN)* and *perspective loss*. DPLN is a sub-network that utilizes all pooling outputs, and the perspective loss reflects DPLN’s result to make a regularization effect. Finally, the CNN model based on SoM-TP forms fine representations through diverse pooling selection, allowing it to capture both the ‘global’ and ‘local’ features of the dataset.

Recognizing the crucial role of pooling in selecting the most representative values from encoded features in CNNs, we have chosen CNNs as the suitable model for our study. We apply our new selection ensemble pooling to Fully Convolutional Networks (FCNs) and Residual Networks (ResNet), which show competitive performances in TSC as a CNN-based model (Wang, Yan, and Oates 2017; Ismail Fawaz et al. 2019). SoM-TP outperforms the exist-

^{*}These authors contributed equally.

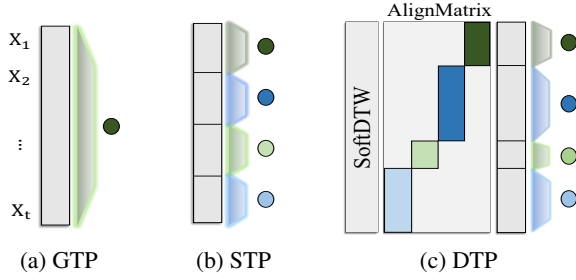


Figure 1: Perspectives of Temporal Poolings. Depending on segmentation types, each temporal pooling generates different pooling outputs and has different *perspectives*.

ing temporal pooling methods and state-of-the-art models of TSC both in univariate and multivariate time series datasets from massive UCR/UEA repositories. We also provide a detailed analysis of the diverse perspective learning result by Layer-wise Relevance Propagation (LRP) (Bach et al. 2015) and the dynamic selection process of SoM-TP. To the best of our knowledge, this is the first novel approach to pooling-level ensemble study in TSC.

Therefore, our contributions are as follows:

- We investigate data dependency arising from distinct perspectives of existing temporal poolings.
- We propose SoM-TP, a new temporal pooling method that fully utilizes the diverse temporal pooling mechanisms through an MCL-inspired selection ensemble.
- We employ an attention mechanism to enable a non-iterative ensemble in a single classifier.
- We define DPLN and perspective loss as a regularizer to promote diverse pooling selection.

Background

Different Perspectives between Temporal Poolings

Convolutional Neural Network in TSC In TSC, CNN outperforms conventional methods, such as nearest neighbor classifiers (Yuan et al. 2019) or COTE (Bagnall et al. 2015; Lines, Taylor, and Bagnall 2016), by capturing local patterns of time series (Ismail Fawaz et al. 2019).

The TSC problem is generally formulated as follows: a time series data $\mathbf{T} = \{(\mathbf{X}_1, y_1), \dots, (\mathbf{X}_t, y_t)\}$, where $\mathbf{X} \in \mathbb{R}^{d \times t}$ of length t with d variables and $y \in \{1, \dots, C\}$ from C classes. Then the convolution stack Φ of out channel dimension k encodes features as hidden representations with temporal position information $\mathbf{H} = \{h_0, \dots, h_t\} \in \mathbb{R}^{k \times t}$ (Lee, Lee, and Yu 2021; Wang, Yan, and Oates 2017).

$$\mathbf{H} = \Phi(\mathbf{T}) \quad (1)$$

After convolutional layers, global pooling plays a key role with two primary purposes: 1) reducing the number of parameters for computational efficiency and preventing overfitting, and 2) learning position invariance. For this purpose, pooling combines the high-dimensional feature outputs into low-dimensional representations (Gholamalinezhad and Khosravi 2020). However, global pooling

presents an issue of losing temporal information, which has led to the development of temporal pooling methods (Lee, Lee, and Yu 2021). We investigate different mechanisms of temporal poolings, which we refer to as *perspective*.

Global Temporal Pooling GTP pools only one representation $\mathbf{p}_g = [p_1] \in \mathbb{R}^{k \times 1}$ in the entire time range. GTP ignores temporal information by aggregating the \mathbf{H} to $\mathbf{p}_g = h$: the global view.

$$\mathbf{p}_g = \text{pool}_g(\mathbf{H}) \quad (2)$$

GTP effectively captures globally dominant features, such as trends or the highest peak, but has difficulty capturing multiple points dispersed on a time axis. To solve this constraint, temporal poolings based on sequential segmentation have been proposed: STP and DTP (Lee, Lee, and Yu 2021). Both have multiple local segments with the given number $n \in \mathbb{Z}^+$: the local view.

Static Temporal Pooling STP divides the time axis equally into n segments with a length $\ell = \frac{t}{n}$, where $\bar{\mathbf{H}} = \{\mathbf{h}_{0:\ell}, \mathbf{h}_{\ell:2\ell}, \dots, \mathbf{h}_{(n-1)\ell:n\ell}\}$ and $\mathbf{p}_s = [p_1, \dots, p_n] \in \mathbb{R}^{k \times n}$. Note that \mathbf{h}_ℓ retains temporal information, but there is no consideration of the temporal relationship between time series in the segmentation process: the uniform local view.

$$\mathbf{p}_s = \text{pool}_s(\bar{\mathbf{H}}) \quad (3)$$

STP functions well on a recursive pattern, such as a stationary process. However, forced uniform segmentation can divide important consecutive patterns or create unimportant segmentations. This inefficiency causes representation power to be distributed to non-informative regions.

Dynamic Temporal Pooling DTP is a learnable pooling layer optimized by soft-DTW (Cuturi and Blondel 2017) for dynamic segmentation considering the temporal relationship. By using the soft-DTW layer, \mathbf{H} is segmented in diverse time lengths $\bar{\ell} = [\ell_1, \ell_2, \dots, \ell_n]$, where $t = \sum \bar{\ell}$. Finally, the optimal pooled vectors $\mathbf{p}_d = [p_{\ell_1}, \dots, p_{\ell_n}] \in \mathbb{R}^{k \times n}$ are extracted from each segment of $\bar{\mathbf{H}}_{\bar{\ell}}$, where $\bar{\mathbf{H}}_{\bar{\ell}} = \{\mathbf{h}_{\ell_1}, \mathbf{h}_{\ell_2}, \dots, \mathbf{h}_{\ell_n}\}$; the dynamic local view.

$$\mathbf{p}_d = \text{pool}_d(\bar{\mathbf{H}}_{\bar{\ell}}) \quad (4)$$

DTP has the highest complexity in finding different optimal segmentation lengths, enabling the pooling to fully represent segmentation power. However, since DTP is based on temporally aligned similarity of hidden features with a constraint that a single time point should not be aligned with multiple consecutive segments, the segmentation can easily divide informative change points that need to be preserved in time series patterns (Appendix. DTP Algorithm).

Limitation of Single Perspective Traditional temporal pooling methods only focus on a single perspective when dealing with hidden features \mathbf{H} . A global perspective cannot effectively capture multiple classification points, while a local perspective struggles to emphasize a dominant classification point. Consequently, datasets that require the simultaneous capture of dominant and hidden local features from diverse viewpoints inevitably exhibit lower performance when using a single perspective. Motivated by these limitations, we propose a novel pooling approach that fully leverages diverse perspectives.

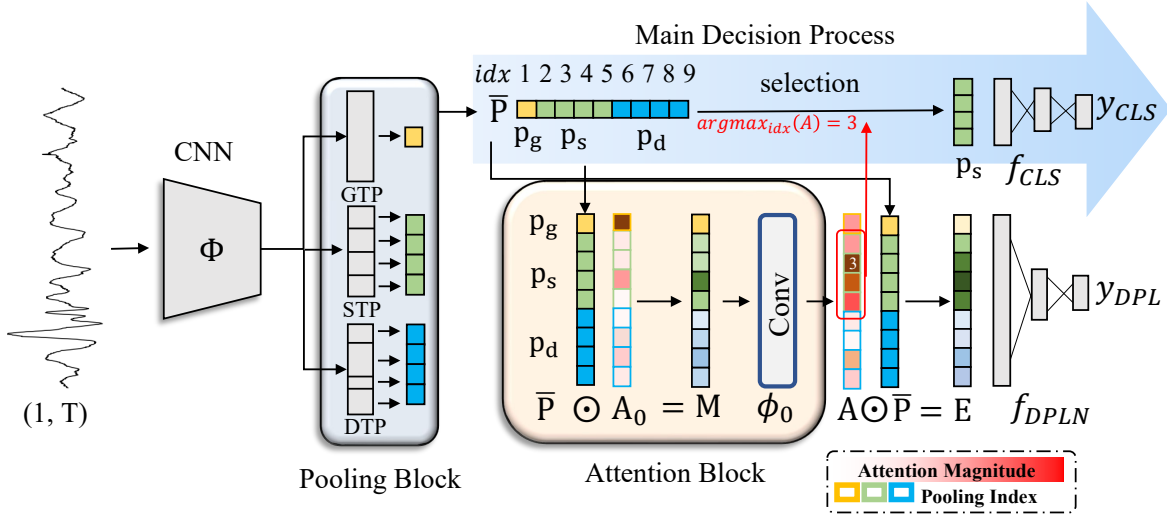


Figure 2: SoM-TP Architecture. Diverse Perspective Learning based on selection-ensemble is achieved as follows: The aggregated output of all pooling, $\bar{\mathbf{P}}$ is passed to the attention block to calculate the attention score \mathbf{A} . In the attention block, a weighted pooling output \mathbf{M} is formed by the multiplication of $\bar{\mathbf{P}}$ and a learnable weight vector \mathbf{A}_0 . After \mathbf{M} passes through the convolutional layer ϕ_0 , the attention score \mathbf{A} is drawn out as an encoded weight vector. Using the index of the highest attention score (here, index 3), pooling for the CLS network is selected. Next, the parameters are updated with the following procedure: 1) DPLN uses the ensembled vector \mathbf{E} , whereas CLS network uses only the selected pooling output (here, \mathbf{p}_s); 2) Each network predicts y_{CLS} and y_{DPLN} respectively, and y_{DPLN} is used in the perspective loss to work as a regularizer; 3) With these two outputs, the model is optimized with diverse perspectives while selecting the proper pooling method for each batch.

Multiple Choice Learning for Deep Temporal Pooling

The traditional ML-based ensemble method focuses on aggregating multiple outputs. However, the aggregation of the simple ensemble makes outputs smoother, due to the generalization effect (Lee et al. 2017). To solve this limitation, MCL has been proposed as an advanced ensemble method that selects the best among multiple outputs using oracle loss (Guzmán-rivera, Batra, and Kohli 2012). More formally, MCL generates M solutions $\hat{Y}_i = (\hat{y}_i^1, \dots, \hat{y}_i^M)$, and learns a mapping $g : \mathcal{X} \rightarrow \mathcal{Y}^M$ that minimizes oracle loss $\min_m \ell(y_i, \hat{y}_i^m)$. The ensemble mapping function g consists of multiple predictors, $g(x) = \{f_1(x), f_2(x), \dots, f_M(x)\}$ (Lee et al. 2016).

The effects of diverse solution sets in MCL can be summarized as addressing situations of ‘Ambiguous evidence’ and ‘Bias towards the mode’. ‘Ambiguous evidence’ refers to situations with insufficient information to make a definitive prediction. In such cases, presenting a small set of reasonable possibilities can alleviate the over-confidence problem of deep learning (Nguyen, Yosinski, and Clune 2015), rather than striving for a single accurate answer. The other situation is ‘Bias towards the mode’, indicating the model’s tendency to learn a mode-seeking behavior to reduce the expected loss across the entire dataset. When only a single prediction exists, the model eventually learns to minimize the average error. In contrast, MCL generates multiple predictions, allowing some classifiers to cover the lower-density regions of the solution space without sacrificing per-

formance on the high-density regions (Lee et al. 2016).

MCL faces computational challenges in deep networks due to the iterative optimization process of the oracle loss, with a complexity of $\mathcal{O}(N^2)$. Although sMCL has partially alleviated this issue through stochastic gradient descent, the method still requires identifying the best output among multiple possibilities (Lee et al. 2016). CMCL, which is another approach to address MCL’s over-confidence problem, cannot be applied at the feature level due to optimization at the output level (Lee et al. 2017). In summary, the integration of MCL into the pooling level is not feasible due to the structural constraints imposed by the oracle loss design. To overcome this challenge, we establish a model structure to incorporate the concept of MCL into a pooling-level ensemble.

Selection over Multiple Temporal Pooling SoM-TP Architecture and Selection Ensemble

Diverse Perspective Learning (DPL) is achieved by dynamically selecting heterogeneous multiple temporal poolings in a single classifier. The overview architecture, as illustrated in Figure 2, consists of four parts: 1) a common feature extractor with CNN Φ ; 2) a pooling block with multiple temporal pooling layers; 3) an attention block with an attention weight vector \mathbf{A}_0 , and a convolutional layer ϕ_0 , as well as 4) Fully Connected layers (FC): a classification network (CLS) f_{CLS} and a DPLN f_{DPLN} . Through these modules, SoM-TP can cover the high probability prediction space, which is aligned with MCL where multiple classifiers are trained to distinguish specific distributions (Lee et al. 2016).

DPL Attention SoM-TP ensembles multiple temporal pooling within a single classifier. The advantage of using a single classifier lies in the absence of the need to compare prediction outputs, making it non-iterative and computationally efficient, in contrast to MCL. Through the attention mechanism (Vaswani et al. 2017), we achieve a ‘comparison-free’ ensemble by dynamically selecting the most suitable temporal pooling for each batch.

DPL attention is an extended attention mechanism that simultaneously considers two factors: the overall dataset and each data sample. In Figure 2, the attention weight vector \mathbf{A}_0 is learned in the direction of adding weight to specific pooling, which has a minimum loss for every batch. Consequently, \mathbf{A}_0 has a weight that reflects the entire dataset.

Next, a convolutional layer ϕ_0 is used to reflect a more specific data level. As shown in Algorithm 1, the weighted pooling vector \mathbf{M} which is the element-wise multiplication between \mathbf{A}_0 and $\bar{\mathbf{P}}$ is given as an input to ϕ_0 . By encoding \mathbf{M} through ϕ_0 , \mathbf{A} can reflect more of each batch characteristic, not just following the dominant pooling in terms of the entire dataset. As a result, this optimized pooling selection by attention can solve the ‘Bias towards the mode’ problem by assigning the most suitable pooling for each data batch, which is aligned with learning the multiple experts in MCL.

Diverse Perspective Learning Network and Perspective Loss

To optimize DPL attention, we introduce DPLN and perspective loss. DPLN is a sub-network that utilizes the weighted aggregation ensemble \mathbf{E} . The main role of DPLN is regularization through perspective loss. In contrast, the CLS network, which predicts the main decision, does not directly utilize attention \mathbf{A} . Instead, it employs a chosen pooling feature output (denoted as \mathbf{p}_s in Figure 2), determined by the index with the biggest score in \mathbf{A} .

Perspective Loss Perspective loss serves as a cost function to maximize the utilization of the sub-network, DPLN, through network tying between the two FC networks. Ultimately, it aims to prevent the CLS network from converging to one dominant pooling and to maintain the benefits of ensemble learning continuously.

To achieve its purpose, perspective loss is designed as the sum of DPLN cross-entropy loss and the Kullback-Leibler (KL) divergence between y_{CLS} and y_{DPL} . Specifically, KL divergence works similarly to CMCL’s KL term, which regulates one model to be over-confident through a uniform distribution, while the KL term of perspective loss regulates based on DPLN (Lee et al. 2017).

$$\begin{aligned}
 KL(y_{CLS}, y_{DPL}) &= y_{DPL} \cdot \log \frac{y_{DPL}}{y_{CLS}}, \\
 \mathcal{L}_{DPLN}(\{\mathcal{W}_\Phi\}, \{\mathbf{W}^{(dpln)}\}) &= -\frac{1}{t} \sum_{n=1}^t \log P(y = y_n | \mathbf{X}_n), \\
 \mathcal{L}_{perspective} &= KL(y_{CLS}, y_{DPL}) + \mathcal{L}_{DPLN},
 \end{aligned} \tag{5}$$

Algorithm 1: SoM-TP selecting algorithm

Function Attention Block (\mathbf{H}):

- ▷ select proper temporal pooling by attention $\mathbf{A} \in \mathbb{R}^{1 \times 3n}$
- ▷ attention weight $\mathbf{A}_0 \in \mathbb{R}^{1 \times 3n}$ is initialized as zero
- ▷ GTP, STP, DTP: $pool_g, pool_s, pool_d$
- ▷ convolutional encoding layer: ϕ_0

Function Pooling Block ($\bar{\mathbf{H}}$):

- ▷ convolutional hidden feature: $\mathbf{H} \in \mathbb{R}^{k \times t}$

- ▷ static segmented hidden feature:

$$\bar{\mathbf{H}} = \{\mathbf{h}_{0:\ell}, \mathbf{h}_{\ell:2\ell}, \dots, \mathbf{h}_{(n-1)\ell:n\ell}\}, \ell = \frac{t}{n}$$

- ▷ dynamic segmented hidden feature:

$$\bar{\mathbf{H}}_{\bar{\ell}} = \{\mathbf{h}_{\ell_1}, \mathbf{h}_{\ell_2}, \dots, \mathbf{h}_{\ell_n}\},$$

$$\bar{\ell} = [\ell_1, \ell_2, \dots, \ell_n], \text{ where } \mathbf{t} = \sum \bar{\ell}$$

- ▷ pooling outputs:

$$\mathbf{p}_g, \mathbf{p}_s, \mathbf{p}_d = pool_g(\mathbf{H}), pool_s(\bar{\mathbf{H}}), pool_d(\bar{\mathbf{H}}_{\bar{\ell}})$$

return $\mathbf{p}_g, \mathbf{p}_s, \mathbf{p}_d$

$$\bar{\mathbf{P}} = [\mathbf{p}_g, \mathbf{p}_s, \mathbf{p}_d]$$

$$\mathbf{M} = \mathbf{A}_0 \odot \bar{\mathbf{P}}$$

$$\mathbf{A} = \phi_0(\mathbf{M}), \text{ where } x \in \mathbf{A}$$

$$idx = \begin{cases} \operatorname{argmax}_i(y), & \text{where } y_i = \frac{\exp(x_i)}{\sum_{i=1}^n \exp(x_i)} \\ \operatorname{argmax}_j(y), & \text{where } y_j = \frac{x_{(j/n)}}{n} \end{cases}$$

return $\mathbf{p} = \bar{\mathbf{P}}(idx), \mathbf{E} = \mathbf{A} \odot \bar{\mathbf{P}}$

where input time series $\{(\mathbf{X}_1, y_1), \dots, (\mathbf{X}_t, y_t)\}$, Φ with learnable parameter \mathcal{W}_Φ of CNN, $y_{CLS} \in \mathbb{R}^{1 \times c}$ from the ‘CLS network’ $\mathbf{W}^{(cls)}$, and $y_{DPL} \in \mathbb{R}^{1 \times c}$ from the DPLN $\mathbf{W}^{(dpln)}$. Then, we set first f_{DPLN} weight matrix $\mathbf{W}_0^{(dpln)} = [\mathbf{w}_1^{(p_g)}, \dots, \mathbf{w}_2^{(p_s)}, \dots, \mathbf{w}_3^{(p_d)}] \in \mathbb{R}^{k \times 3 \cdot n}$, where $\mathbf{w}^{(p)} \in \mathbb{R}^k$ is weight matrix of each latent dimension k of pooling \mathbf{p}_i , whereas $\mathbf{W}_0^{(cls)} = [\mathbf{w}_1^{(c)}, \dots, \mathbf{w}_n^{(c)}] \in \mathbb{R}^{k \times n}$ is the first f_{CLS} weight matrix (Lee, Lee, and Yu 2021). Note that the results of GTP are repeated n times to give the same proportion for each pooling by attention weight.

Therefore, the final loss function of the SoM-TP is designed as follows,

$$\begin{aligned}
 \mathcal{L}_{CLS}(\{\mathcal{W}_\Phi\}, \{\mathbf{W}^{(cls)}\}) &= -\frac{1}{t} \sum_{n=1}^t \log P(y = y_n | \mathbf{X}_n), \\
 \mathcal{L}_{cost}(\{\mathcal{W}_\Phi\}, \{\mathbf{W}\}) &= \mathcal{L}_{CLS} + \lambda \cdot \mathcal{L}_{perspective},
 \end{aligned} \tag{6}$$

where $\{\mathbf{W}^{(cls)}, \mathbf{W}^{(dpln)}, \mathbf{A}_0, \phi_0\} \in \mathbf{W}$ are learnable parameters. Prioritizing classification accuracy, the loss \mathcal{L}_{CLS} is computed, and $\mathcal{L}_{perspective}$ is added with λ decay.

As a result, SoM-TP can address the ‘Ambiguous evidence’ problem through DPLN and perspective loss. In a pooling ensemble, the ‘Ambiguous evidence’ can be conceived as a scenario where a single pooling is not dominant. Even though SoM-TP selects only one pooling, y_{DPL} in the perspective loss enables the model to consider the importance of other poolings.

CNN	POOL (type)	UCR (uni-variate)					UEA (multi-variate)				
		ACC	F1 macro	ROC AUC	PR AUC	Rank	ACC	F1 macro	ROC AUC	PR AUC	Rank
FCN	MAX										
	GTP	0.6992	0.6666	0.8662	0.7406	3.6	0.6558	0.6213	0.7841	0.6854	3.9
	STP	<u>0.7462</u>	<u>0.7133</u>	<u>0.8924</u>	<u>0.7889</u>	<u>2.7</u>	<u>0.6801</u>	<u>0.6603</u>	0.8001	0.6984	<u>3.0</u>
	DTP euc	0.7406	0.7123	0.8897	0.7782	3.1	0.6795	0.6559	<u>0.8129</u>	<u>0.7163</u>	3.4
	DTP cos	0.7335	0.7062	0.8879	0.7768	2.9	0.6702	0.6314	0.8061	0.7022	3.1
SoM-TP	0.7556	0.7241	0.9026	0.8000	2.6	0.6920	0.6621	0.8105	0.7099	2.4	
ResNet	GTP	0.7227	0.6952	0.8837	0.7654	3.5	0.6423	0.6083	0.7798	0.6769	3.5
	STP	0.7420	0.7126	0.8880	0.7864	<u>2.9</u>	<u>0.6717</u>	<u>0.6383</u>	0.7962	0.6934	<u>2.8</u>
	DTP euc	0.7456	0.7197	0.8939	0.7846	3.0	0.6567	0.6271	<u>0.7981</u>	<u>0.6968</u>	3.1
	DTP cos	0.7452	0.7198	<u>0.8945</u>	0.7829	3.0	0.6534	0.6377	0.7895	0.6832	3.0
	SoM-TP	0.7773	0.7489	0.9182	0.8261	2.4	0.6769	0.6387	0.8016	0.7033	2.5

*This table is for SoM-TP pooling selection operation type MAX.

Table 1: SoM-TP Comparison with Single Perspective Temporal Poolings. The table presents the effectiveness of the selection ensemble of SoM-TP compared to traditional temporal poolings on operation type MAX. The best performances where SoM-TP outperforms others are bolded, and the best performances of other temporal poolings are underlined.

Optimization

For attention weight \mathbf{A}_0 , SoM-TP proceeds with additional optimization: a dot product similarity to regulate \mathbf{A}_0 . The similarity term is defined as,

$$\mathcal{L}_{attn} = -y_{CLS} \cdot y_{DPL}, \quad (7)$$

Due to the KL-divergence cost function in perspective loss, the CLS network and DPLN can be overly similar during the optimization process. As the additional regulation for output over-similarity, \mathcal{L}_{attn} plays the opposite regulation to the perspective loss. Note that the dot-product similarity considers both the magnitude and direction of two output vectors.

Finally, the overall optimization process is as follows,

$$\begin{aligned} \mathbf{A}_0 &\leftarrow \mathbf{A}_0 - \eta \cdot \partial \mathcal{L}_{attn} / \partial \mathbf{A}_0, \\ \mathcal{W}_\Phi &\leftarrow \mathcal{W}_\Phi - \eta \cdot \partial \mathcal{L}_{cost} / \partial \mathcal{W}_\Phi, \\ \mathbf{W} &\leftarrow \mathbf{W} - \eta \cdot \partial \mathcal{L}_{cost} / \partial \mathbf{W}. \end{aligned} \quad (8)$$

As a result, even with a non-iterative optimization process, SoM-TP learns various perspectives through DPL attention, DPLN, and perspective loss. Consequently, Φ reflects f_{CLS} and f_{DPLN} relatively while minimizing the similarity between each network output.

Experiments

Experimental Settings

For the extensive evaluation, 112 univariate and 22 multivariate time series datasets from the UCR/UEA repositories are used (Bagnall et al. 2018; Dau et al. 2019); collected from a wide range of domains and publicly available. To ensure the validity of our experiments, we exclude a few datasets from the UCR/UEA repositories due to the irregular data lengths. While zero padding could resolve this, it might cause bias in some time series models.

All temporal pooling methods have the same CNN architecture. FCN and ResNet are specifically designed as a feature extractor (Wang, Yan, and Oates 2017), and temporal poolings are constructed with the same settings: normalization with BatchNorm (Ioffe and Szegedy 2015), activation

function with ReLU, and optimizer with Adam (Kingma and Ba 2015). The validation set is made from 20% of the training set for a more accurate evaluation. In the case of imbalanced classes, a weighted loss is employed. The prototype number n is searched in a greedy way, taking into consideration the unique class count of each dataset. Specifically, we observe that selecting 4-10 segments based on the class count in each dataset enhances performance. Consequently, we use an equal number of segments in each dataset for segment-based poolings (Appendix. Table 5).

Baselines We conduct two experiments to evaluate the performance of SoM-TP. First, we compare it with traditional temporal poolings, GTP, STP, and DTP, to demonstrate the effectiveness of selection-ensemble in temporal poolings (Lee, Lee, and Yu 2021). Second, we compare SoM-TP with other state-of-the-art models that utilize advanced methods, including scale-invariant methods (ROCKET (Dempster, Petitjean, and Webb 2020), InceptionTime (Ismail Fawaz et al. 2020), OS-CNN (Tang et al. 2021), and DSN (Xiao et al. 2022)), sequential models (MLSTM-FCN (Karim et al. 2019), and TCN (Bai, Kolter, and Koltun 2018)), and Transformer-based models (Vanilla-Transformer (Vaswani et al. 2017), TST (Zerveas et al. 2021), and ConvTran (Foumani et al. 2024)). Models leveraging temporal information use attention or RNNs to emphasize long-term dependencies. On the other hand, scale-invariant learning models employ a CNN-based architecture with various kernel sizes to find the optimum through global average pooling.

Experimental Evaluation

Performance Analysis As shown in Table 1, SoM-TP shows superior performance for overall TSC datasets when compared to conventional temporal poolings. We calculate the average performance of the entire repository. We consider not only accuracy but also the F1 macro score, ROC-AUC, and PR-AUC to consider the imbalanced class. Quantitatively, SoM-TP outperforms the existing temporal pooling methods both in univariate and multivariate time series datasets. Through these results, we can confirm that the dynamic selection ensemble of SoM-TP boosts the performance of the CNN model.

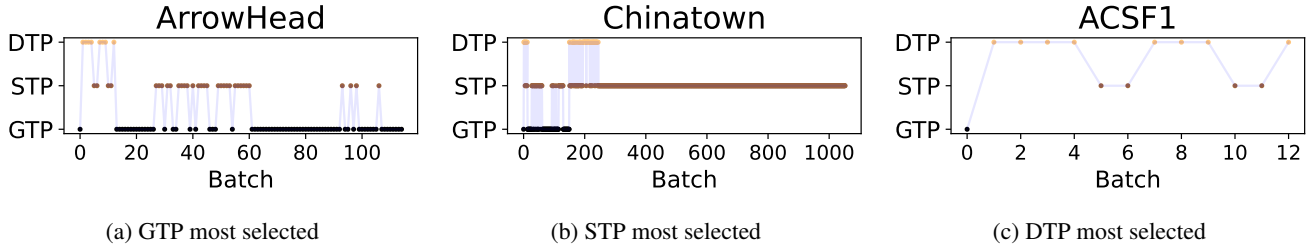


Figure 3: Dynamic Pooling Selection in SoM-TP. This figure represents the graph of dynamic selection in the FCN SoM-TP MAX on the UCR repository: ArrowHead, Chinatown, and ACSF1.

Methods	UCR				UEA			
	Baseline	SoM-TP wins	Tie	Rank	Baseline	SoM-TP wins	Tie	Rank
Vanilla-Transformer (Vaswani et al. 2017)	10	99	4	5.2	3	18	1	4.4
TCN (Bai, Kolter, and Koltun 2018)	28	80	5	4.0	4	17	1	4.3
TST (Zerveas et al. 2021)	32	78	3	3.8	6	15	1	3.6
ConvTran (Foumani et al. 2024)	35	71	7	3.1	8	13	1	3.1
MLSTM-FCN (Karim et al. 2019)	46	60	6	2.6	6	12	4	3.2
SoM-TP - MAX	-	-	-	2.5	-	-	-	2.5

Methods	UCR				UEA			
	Acc	F1-score	ROC AUC	PR AUC	Acc	F1-score	ROC AUC	PR AUC
ROCKET (Dempster, Petitjean, and Webb 2020)	<u>0.7718</u>	<u>0.7478</u>	0.8899	0.7841	0.6785	<u>0.6592</u>	0.7926	0.6940
InceptionTime (Ismail Fawaz et al. 2020)	0.7713	0.7455	<u>0.9056</u>	0.8164	0.6612	0.6360	0.7984	<u>0.7106</u>
OS-CNN (Tang et al. 2021)	0.7663	0.7324	0.9005	0.8139	<u>0.6808</u>	0.6547	0.8118	0.7137
DSN (Xiao et al. 2022)	0.7488	0.7230	0.8838	0.7968	0.5648	0.5433	0.7575	0.6265
SoM-TP - MAX	0.7773	0.7489	0.9182	0.8261	0.6920	0.6621	<u>0.8105</u>	0.7099

Table 2: SoM-TP Comparison with Advanced TSC Methods. This table compares the performance of SoM-TP with advanced TSC models that leverage temporal information and those that exploit scale-invariant properties, respectively. The best performances, where SoM-TP beat others, are bolded, and the best performances among other models are underlined.

Type	SoM-TP Modules				Rank			Acc
	A_0	ϕ_0	DPLN	\mathcal{L}_{attn}	1	2	3	
only ϕ_0		✓			8	15	17	0.6966
only A_0	✓				4	9	24	0.6963
DPL Attention	✓	✓			6	7	23	0.6974
DPLN w/o A_0		✓	✓		6	14	29	0.7047
DPLN	✓	✓	✓		23	27	26	0.7399
SoM-TP	✓	✓	✓	✓	42	20	6	0.7503

Table 3: SoM-TP Module Ablation Study.

Additionally, Table 2 compares SoM-TP with other state-of-the-art TSC models from two different approaches. In Table 2-1, ResNet SoM-TP MAX significantly outperforms other sequential models in terms of comparing models leveraging temporal information. As SoM-TP clearly outperforms all other models in accuracy metric, we demonstrate the robustness of performance by providing the number of datasets where SoM-TP achieves higher accuracy. Considering the lowest average rank of SoM-TP, we can conclude that dynamic pooling selection leverages the model to keep important temporal information in a more optimal way than other methods in the massive UCR/UEA repository.

Next, Table 2-2 highlights SoM-TP’s comparable perfor-

mance alongside scale-invariant methods, even with SoM-TP’s significant computational efficiency. Since SoM-TP and scale-invariant methods have different learning approaches, it is suitable to consider various metrics. Regarding the time complexity of models, scale-invariant methods consider various receptive fields of a CNN, which results in longer training times. In contrast, SoM-TP achieves comparable performance with only one-third of the time.

Finally, in Table 3, we present the results of an ablation study on the modules of SoM-TP discussed in Section 3. When each module, including A_0 and ϕ_0 constituting DPL Attention, DPLN, and \mathcal{L}_{attn} , is removed, it decreases SoM-TP’s performance. In terms of dataset robustness, we can observe through the rank results that all modules contribute to promoting SoM-TP’s Diverse Perspective Learning.

Perspective Analysis with LRP In Figure 3, we can observe that SoM-TP dynamically selects pooling during inference. ArrowHead, Chaintown, and ACSF1, in order, are datasets where GTP, STP, and DTP pooling selections are most frequently chosen. The DPL attention is trained to select the optimal pooling for each batch during the training process, and during inference, it continues to choose the most suitable pooling without DPLN (Appendix. Figure 7).

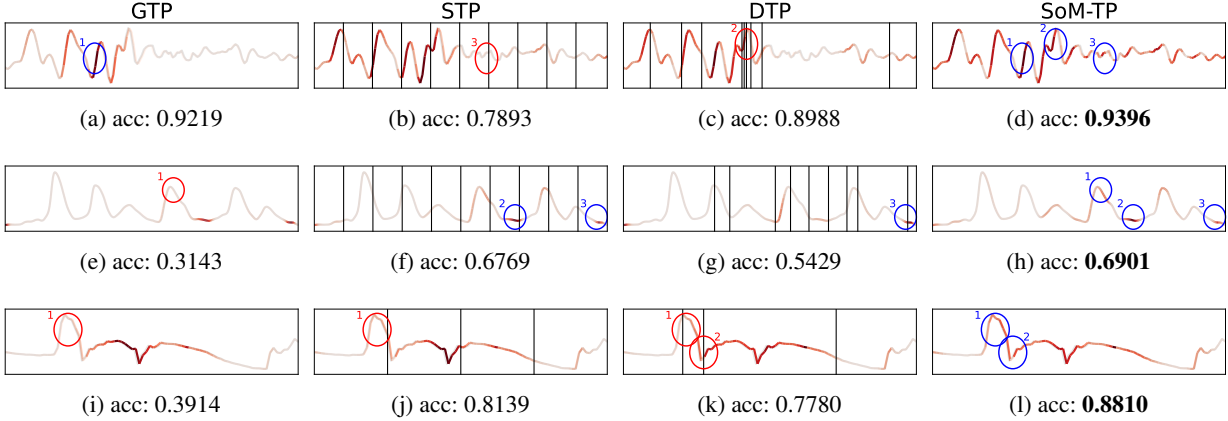


Figure 4: Comparison of LRP Input Attribution on Single vs Diverse Perspective Learning. The figure shows LRP attribution results for FaceAll, FiftyWords, and MoteStrain datasets in the UCR repository, ordered in respective rows. Pooling choice significantly affects accuracy and attributions, reflecting different perspectives. Redder areas of time series indicate higher attribution, aligning with LRP’s conservation rule of summing to 1. Blue circles denote well-captured regions, while red circles suggest dispersed focus or inadequate capture. Given the absence of a ground truth concept for input attributes in TSC, we infer these implicitly from the presented accuracy.

Model	Complexity	
	Pooling	Optimization
GTP	$\mathcal{O}(1)$	$\mathcal{O}(N)$
STP/DTP	$\mathcal{O}(L)$	
SoM-TP	$\mathcal{O}(L_P) + \mathcal{O}(L_{mul}) = \mathcal{O}(L)$	
MCL	-	$\mathcal{O}(N^2)$

Table 4: Complexity Study.

For qualitative analysis, we employ Layer-wise Relevance Propagation (LRP) to understand how different temporal pooling perspectives capture time series patterns. LRP attributes relevance to input features, signifying their contribution to the output. Note that the conservation rule maintains relevance sum in backward propagation, ensuring that the sum of attribution is 1. We use the LRP z^+ rule for the convolutional stack Φ , and the ϵ rule for the FC layers.

In Figure 4, GTP focuses on globally crucial parts (a, e, i), while STP and DTP use local views within segmented time series for a more balanced representation (b, c, f, g, j, k). However, GTP’s limitation lies in concentrating only on specific parts, neglecting other local aspects (e, i). Conversely, STP and DTP risk diluting the primary representation by reflecting all local segments (b, j) or cutting significant series due to forced segmentation (c, k). DTP often segments at change points, losing essential information (c, k).

SoM-TP addresses these issues by combining global and local views of each pooling method via diverse perspective learning. In Figure 4-(d), SoM-TP captures GTP’s points (d-1) and enhances multiple representations by effectively capturing local patterns (d-2, d-3). In (h), SoM-TP identifies the common important points (h-2, h-3) and complements GTP’s missed local points (h-1). Finally, in (l), SoM-TP captures GTP’s missed local points (l-1) and fully utilizes important time series (l-2) cut by STP and DTP (j-1, k-1, k-2).

Complexity of SoM-TP We compare the complexity of independent temporal poolings: pooling and optimization complexity. We exclude the maximum or average operation, which is common for all pooling complexity.

As shown in Table 4, for the pooling complexity, GTP has $\mathcal{O}(1)$ while STP and DTP have $\mathcal{O}(L)$ from segmenting. SoM-TP has increased complexity as $\mathcal{O}(L_P + L_{mul}) = \mathcal{O}(L)$ for computation of the attention score, where $\mathcal{O}(L_P)$ is for a sum of the three temporal poolings’ complexity, making it $\mathcal{O}(L)$, and $\mathcal{O}(L_{mul})$ for the complexity of multiplication between $\bar{\mathbf{P}}$ and \mathbf{A}_0 , and between $\bar{\mathbf{P}}$ and \mathbf{A} . As for the optimization complexity, SoM-TP and other temporal poolings have all $\mathcal{O}(N)$, while MCL has $\mathcal{O}(N^2)$ to generate and compare multiple outputs. Therefore, compared with independent pooling, SoM-TP has little degradation of complexity, while optimization is effectively achieved even with an ensemble.

Conclusion

This paper proposes SoM-TP, a novel temporal pooling method employing a selection ensemble to address data dependency in temporal pooling by learning diverse perspectives. Utilizing a selection ensemble inspired by MCL, SoM-TP adapts to each data batch’s characteristics. Optimal pooling selection with DPL attention achieves a comparison-free ensemble. We define DPLN and perspective loss for effective ensemble optimization. In quantitative evaluation, SoM-TP surpasses other pooling methods and state-of-the-art TSC models in UCR/UEA experiments. In qualitative analysis, LRP results highlight SoM-TP’s ability to complement existing temporal pooling limitations. We re-examine the conventional role of temporal poolings, identify their limitations, and propose an efficient data-driven temporal pooling ensemble as a first attempt.

Acknowledgements

This work was partly supported by Institute of Information & Communications Technology Planning & Evaluation (IITP) grant funded by the Korea government (MSIT) (No. 2022-0-00984, Development of Artificial Intelligence Technology for Personalized Plug-and-Play Explanation and Verification of Explanation; No. 2022-0-00184, Development and Study of AI Technologies to Inexpensively Conform to Evolving Policy on Ethics; No. 2021-0-02068, Artificial Intelligence Innovation Hub; No. 2019-0-00075, Artificial Intelligence Graduate School Program (KAIST)).

References

- Alsallakh, B.; Yan, D.; Kokhlikyan, N.; Miglani, V.; Reblitz-Richardson, O.; and Bhattacharya, P. 2023. Mind the Pool: Convolutional Neural Networks Can Overfit Input Size. In *Proceedings of the 11th International Conference on Learning Representations (ICLR'23)*.
- Bach, S.; Binder, A.; Montavon, G.; Klauschen, F.; Müller, K.-R.; and Samek, W. 2015. On Pixel-Wise Explanations for Non-Linear Classifier Decisions by Layer-Wise Relevance Propagation. *PLOS ONE*, 10(7): 1–46.
- Bagnall, A.; Dau, H. A.; Lines, J.; Flynn, M.; Large, J.; Bostrom, A.; Southam, P.; and Keogh, E. 2018. The UEA multivariate time series classification archive, 2018. arXiv:1811.00075.
- Bagnall, A.; Lines, J.; Hills, J.; and Bostrom, A. 2015. Time-Series Classification with COTE: The Collective of Transformation-Based Ensembles. *IEEE Transactions on Knowledge and Data Engineering*, 27(9): 2522–2535.
- Bai, S.; Kolter, J. Z.; and Koltun, V. 2018. An Empirical Evaluation of Generic Convolutional and Recurrent Networks for Sequence Modeling. arXiv:1803.01271.
- Bay, S. D.; Kibler, D.; Pazzani, M. J.; and Smyth, P. 2000. The UCI KDD archive of large data sets for data mining research and experimentation. *ACM SIGKDD Explorations Newsletter*, 2(2): 81–85.
- Cui, Z.; Chen, W.; and Chen, Y. 2016. Multi-scale convolutional neural networks for time series classification. arXiv preprint arXiv:1603.06995.
- Cuturi, M.; and Blondel, M. 2017. Soft-DTW: A Differentiable Loss Function for Time-Series. In *Proceedings of the 34th International Conference on Machine Learning (ICML'17)*.
- Dau, H. A.; Bagnall, A.; Kamgar, K.; Yeh, C.-C. M.; Zhu, Y.; Gharghabi, S.; Ratanamahatana, C. A.; and Keogh, E. 2019. The UCR time series archive. *IEEE/CAA Journal of Automatica Sinica*, 6(6): 1293–1305.
- Dempster, A.; Petitjean, F.; and Webb, G. I. 2020. ROCKET: Exceptionally Fast and Accurate Time Series Classification Using Random Convolutional Kernels. *Data Mining and Knowledge Discovery*, 34(5): 1454–1495.
- Esling, P.; and Agon, C. 2012. Time-Series Data Mining. *ACM Comput. Surv.*, 45(1).
- Foumani, N. M.; Tan, C. W.; Webb, G. I.; and Salehi, M. 2024. Improving position encoding of transformers for multivariate time series classification. *Data Mining and Knowledge Discovery*, 38(1): 22–48.
- Gao, Z.; Wang, Q.; Zhang, B.; Hu, Q.; and Li, P. 2021. Temporal-attentive covariance pooling networks for video recognition. In *Proceedings of the 35th Advances in Neural Information Processing Systems (NIPS'21)*.
- Gholamalizadeh, H.; and Khosravi, H. 2020. Pooling Methods in Deep Neural Networks, a Review. arXiv:2009.07485.
- Girdhar, R.; and Ramanan, D. 2017. Attentional pooling for action recognition. In *Proceedings of the 31st Advances in Neural Information Processing Systems (NIPS'17)*.
- Guzmán-rivera, A.; Batra, D.; and Kohli, P. 2012. In *Proceedings of the 26th Advances in Neural Information Processing Systems (NIPS'12)*.
- Hinton, G. E.; Sabour, S.; and Frosst, N. 2018. Matrix capsules with EM routing. In *Proceedings of the 6th International Conference on Learning Representations (ICLR'18)*.
- Hou, Q.; Zhang, L.; Cheng, M.-M.; and Feng, J. 2020. Strip pooling: Rethinking spatial pooling for scene parsing. In *Proceedings of the IEEE/CVF Conference on Computer Vision and Pattern Recognition (CVPR'20)*.
- Ioffe, S.; and Szegedy, C. 2015. Batch Normalization: Accelerating Deep Network Training by Reducing Internal Covariate Shift. In *Proceedings of the 32nd International Conference on Machine Learning (ICML'15)*.
- Ismail Fawaz, H.; Forestier, G.; Weber, J.; Idoumghar, L.; and Muller, P.-A. 2019. Deep learning for time series classification: a review. *Data Mining and Knowledge Discovery*, 33(4): 917–963.
- Ismail Fawaz, H.; Lucas, B.; Forestier, G.; Pelletier, C.; Schmidt, D. F.; Weber, J.; Webb, G. I.; Idoumghar, L.; Muller, P.-A.; and Petitjean, F. 2020. InceptionTime: Finding AlexNet for Time Series Classification. *Data Mining and Knowledge Discovery*, 34(6): 1936–1962.
- Kachuee, M.; Fazeli, S.; and Sarrafzadeh, M. 2018. ECG Heartbeat Classification: A Deep Transferable Representation. *CoRR*, abs/1805.00794.
- Karim, F.; Majumdar, S.; Darabi, H.; and Harford, S. 2019. Multivariate LSTM-FCNs for time series classification. *Neural Networks*, 116: 237–245.
- Kingma, D. P.; and Ba, J. 2015. Adam: A Method for Stochastic Optimization. In *Proceedings of 3rd International Conference on Learning Representations (ICLR'15)*.
- Lecun, Y.; Bottou, L.; Bengio, Y.; and Haffner, P. 1998. Gradient-based learning applied to document recognition. In *Proceedings of the IEEE*.
- Lee, D.; Lee, S.; and Yu, H. 2021. Learnable Dynamic Temporal Pooling for Time Series Classification. In *Proceedings of the 35th AAAI Conference on Artificial Intelligence (AAAI'21)*.
- Lee, K.; Hwang, C.; Park, K.; and Shin, J. 2017. Confident Multiple Choice Learning. In *Proceedings of the 34th International Conference on Machine Learning (ICML'17)*.

- Lee, S.; Purushwalkam, S.; Cogswell, M.; Ranjan, V.; Crandall, D.; and Batra, D. 2016. Stochastic Multiple Choice Learning for Training Diverse Deep Ensembles. In *Proceedings of the 30th Advances in Neural Information Processing Systems (NIPS'16)*.
- Lines, J.; Taylor, S.; and Bagnall, A. 2016. HIVE-COTE: The Hierarchical Vote Collective of Transformation-Based Ensembles for Time Series Classification. In *Proceedings of the 16th IEEE International Conference on Data Mining (ICDM'16)*.
- Liu, H.; Simonyan, K.; and Yang, Y. 2019. DARTS: Differentiable Architecture Search. In *Proceedings of the 7th International Conference on Learning Representations (ICLR'19)*.
- Långkvist, M.; Karlsson, L.; and Loutfi, A. 2014. A review of unsupervised feature learning and deep learning for time-series modeling. *Pattern Recognition Letters*, 42: 11–24.
- Nguyen, A.; Yosinski, J.; and Clune, J. 2015. Deep neural networks are easily fooled: High confidence predictions for unrecognizable images. In *Proceedings of the IEEE/CVF Conference on Computer Vision and Pattern Recognition (CVPR'15)*.
- Pigou, L.; Van Den Oord, A.; Dieleman, S.; Van Herreweghe, M.; and Dambre, J. 2018. Beyond temporal pooling: Recurrence and temporal convolutions for gesture recognition in video. *International Journal of Computer Vision*, 126: 430–439.
- Rakthanmanon, T.; Campana, B.; Mueen, A.; Batista, G.; Westover, B.; Zhu, Q.; Zakaria, J.; and Keogh, E. 2012. Searching and mining trillions of time series subsequences under dynamic time warping. In *Proceedings of the 18th ACM SIGKDD International Conference on Knowledge Discovery and Data Mining (KDD'12)*.
- Rippel, O.; Snoek, J.; and Adams, R. P. 2015. Spectral representations for convolutional neural networks. In *Proceedings of the 28th Advances in Neural Information Processing Systems (NIPS'15)*.
- Sabour, S.; Frosst, N.; and Hinton, G. E. 2017. Dynamic routing between capsules. In *Proceedings of the 31st Advances in Neural Information Processing Systems (NIPS'17)*.
- Schäfer, P. 2015. The BOSS is concerned with time series classification in the presence of noise. *Data Mining and Knowledge Discovery*, 29: 1505–1530.
- Tan, C. W.; Dempster, A.; Bergmeir, C.; and Webb, G. I. 2022. MultiRocket: multiple pooling operators and transformations for fast and effective time series classification. *Data Mining and Knowledge Discovery*, 36(5): 1623–1646.
- Tang, W.; Long, G.; Liu, L.; Zhou, T.; Blumenstein, M.; and Jiang, J. 2021. Omni-Scale CNNs: a simple and effective kernel size configuration for time series classification. In *Proceedings of the 9th International Conference on Learning Representations (ICLR'21)*.
- Vaswani, A.; Shazeer, N.; Parmar, N.; Uszkoreit, J.; Jones, L.; Gomez, A. N.; Kaiser, L. u.; and Polosukhin, I. 2017. Attention is All you Need. In *Proceedings of the 31st Advances in Neural Information Processing Systems (NIPS'17)*.
- Wang, J.; Shao, Z.; Huang, X.; Lu, T.; Zhang, R.; and Lv, X. 2021. Spatial-temporal pooling for action recognition in videos. *Neurocomputing*, 451: 265–278.
- Wang, Z.; Yan, W.; and Oates, T. 2017. Time series classification from scratch with deep neural networks: A strong baseline. In *Proceedings of the International Joint Conference on Neural Networks (IJCNN'17)*.
- Xiao, Q.; Wu, B.; Zhang, Y.; Liu, S.; Pechenizkiy, M.; Mocanu, E.; and Mocanu, D. C. 2022. Dynamic Sparse Network for Time Series Classification: Learning What to “See”. In *Proceedings of the 36th Advances in Neural Information Processing Systems (NIPS'22)*.
- Yu, D.; Wang, H.; Chen, P.; and Wei, Z. 2014. Mixed Pooling for Convolutional Neural Networks. *Rough Sets and Knowledge Technology*, 364–375.
- Yuan, J.; Douzal-Chouakria, A.; Varasteh Yazdi, S.; and Wang, Z. 2019. A large margin time series nearest neighbour classification under locally weighted time warps. *Knowledge and Information Systems*, 59(1): 117–135.
- Zerveas, G.; Jayaraman, S.; Patel, D.; Bhamidipaty, A.; and Eickhoff, C. 2021. A Transformer-Based Framework for Multivariate Time Series Representation Learning. In *Proceedings of the 27th ACM SIGKDD International Conference on Knowledge Discovery and Data Mining (KDD'21)*.
- Zhang, X.; Gao, Y.; Lin, J.; and Lu, C.-T. 2020. Tapnet: Multivariate time series classification with attentional prototypical network. In *Proceedings of the 34th AAAI Conference on Artificial Intelligence (AAAI'20)*.
- Zhao, P.; Luo, C.; Qiao, B.; Wang, L.; Rajmohan, S.; Lin, Q.; and Zhang, D. 2022. T-SMOTE: Temporal-oriented Synthetic Minority Oversampling Technique for Imbalanced Time Series Classification. In *Proceedings of the 31st International Joint Conference on Artificial Intelligence (IJCAI'22)*.
- Zoph, B.; and Le, Q. 2017. Neural Architecture Search with Reinforcement Learning. In *Proceedings of the 5th International Conference on Learning Representations (ICLR'17)*.

Related Work

Time Series Classification Methods

In recent Time Series Classification (TSC) tasks, deep learning models have shown significant performance improvement (Lee, Lee, and Yu 2021; Wang, Yan, and Oates 2017; Ismail Fawaz et al. 2019), surpassing that of traditional machine learning models such as DTW (Rakthanmanon et al. 2012), BOSS (Schäfer 2015), COTE (Bagnall et al. 2015), and HIVE-COTE (Lines, Taylor, and Bagnall 2016). Various deep learning methodologies have been proposed to address the characteristics of time series, broadly classified into two categories: 1) learning diverse receptive fields using various convolution kernels to handle variant scales of time series, and 2) preserving temporal information to reduce the loss of unique information in time series.

Scale-Invariant Learning Methods Models belonging to scale-invariant methods, such as MCNN (Cui, Chen, and Chen 2016), InceptionTime (Ismail Fawaz et al. 2020), Tapnet (Zhang et al. 2020), ROCKET (Dempster, Petitjean, and Webb 2020; Tan et al. 2022), OS-CNN (Tang et al. 2021), and DSN (Xiao et al. 2022), utilize various convolutional kernels to cover multiple receptive fields and extract relevant features across different time series scales. The incorporation of scale-invariant properties in these models has significantly contributed to the improvement of TSC performance. However, these models are limited to convolutional design, have high computational costs, and can be easily overfitted, particularly when trained on small datasets. In general, finding an adaptive receptive field largely depends on optimal kernel size or masks during training, a process that is sparse and imposes substantial computational costs (Xiao et al. 2022).

Temporal Information Leveraging Methods Recent research has focused on scale-invariant learning through the application of diverse convolution kernels, achieving remarkable results. Despite this progress, we still emphasize the importance of utilizing another crucial feature of time series data: temporal information (Lee, Lee, and Yu 2021; Zhao et al. 2022). One approach to reflect this is to use the CNN structure for TSC, as proposed by Wang, Yan, and Oates (2017), along with FCN and ResNet. These architectures stack CNN layers without pooling to preserve temporal information. However, this information is ultimately lost when global pooling is used in the final layer. Alternatively, some models directly utilize RNN layers, such as MLSTM-FCN (Karim et al. 2019), use a Transformer-based approach like TST (Zerveas et al. 2021), or redesign convolution for sequential modeling, such as TCN (Bai, Kolter, and Koltun 2018). However, sequential models have higher complexity than CNN-based models and are limited to performing well only on time series data with long-term dependencies.

Advanced Temporal Pooling Methods

In CNNs, global pooling is commonly used to reduce dimensionality and computation costs. One of the most frequently used methods is MAX and AVG global pooling, which has demonstrated great success in classification tasks.

However, it has been criticized for its suboptimal information preservation (Sabour, Frosst, and Hinton 2017; Hinton, Sabour, and Frosst 2018). This drawback can be illustrated in two ways. First, global pooling causes a significant decrease in dimensionality, leading to a loss of information in the data. Second, when the MAX operation is used, global pooling only reflects local information and constrains the ability to effectively minimize approximation loss (Rippel, Snoek, and Adams 2015).

To address the issue in time series data, Lee, Lee, and Yu (2021) proposed Dynamic Temporal Pooling (DTP) to mitigate the temporal information loss caused by global pooling in the CNN architecture designed by Wang, Yan, and Oates (2017). DTP employs a soft-DTW (Cuturi and Blondel 2017) layer to cluster similar time segments before pooling. DTP relies on aligning hidden features temporally but imposes a constraint against aligning a single time point with multiple consecutive segments. This constraint in segmentation may lead to the inadvertent separation of crucial change points that are vital for preserving time series patterns. Additionally, another advanced temporal pooling method, MultiRocket (Tan et al. 2022), is tailored specifically to be efficient and scalable within the ROCKET architecture (Dempster, Petitjean, and Webb 2020). Therefore, it poses challenges when attempting to apply it to the pooling layer within a general CNN model architecture.

The pursuit of advanced pooling techniques extends beyond Time Series Classification (TSC) and encompasses diverse domains. For example, researchers are actively exploring ways to preserve image sequence information in pooling for video data (Gao et al. 2021; Girdhar and Ramanan 2017; Pigou et al. 2018; Wang et al. 2021). Similarly, in the image domain, ongoing research aims to maintain spatial information during pooling (Alsallakh et al. 2023; Hou et al. 2020). It is noteworthy that minimizing information loss during the pooling process remains a significant challenge across these diverse domains as well.

Difference between SoM-TP and Neural Architecture Search

Neural Architecture Search (NAS) (Zoph and Le 2017) is a methodology designed to automatically discover optimal or highly effective neural network architectures tailored for specific tasks. In contrast to NAS, which aims to find the most efficient configuration for all modules in the entire model architecture, SoM-TP has a distinct objective: the selection of optimal pooling methods. Even when applying NAS only to the pooling layer, SoM-TP possesses two notable differences from NAS (Liu, Simonyan, and Yang 2019). First, SoM-TP dynamically selects the optimal pooling path for each data batch, while NAS converges towards a fixed path based solely on overall dataset performance. Second, in terms of optimization, NAS faces a bilevel optimization problem to identify the path for the entire network, while SoM-TP optimizes a single classifier by utilizing the sub-network (DPLN) loss as a regularizer. In summary, SoM-TP has clear differences from NAS in terms of convergence and optimization.

Extended Analysis on SoM-TP

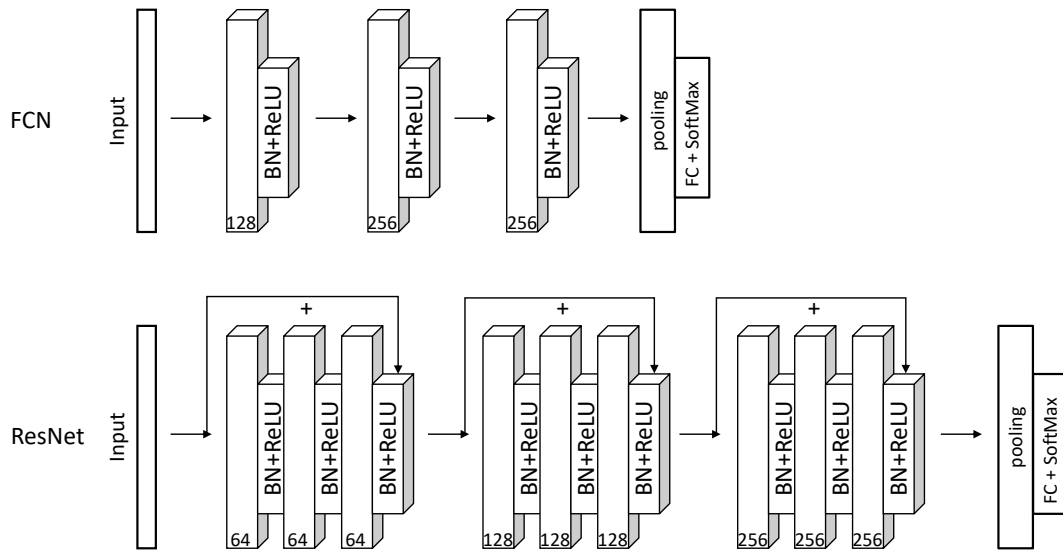


Figure 5: **Convolutional Stack Architectures.** The overall architectures of FCN and ResNet used in this paper follow the baseline models presented by Wang, Yan, and Oates (2017), specifically designed for Time Series Classification (TSC). In both architectures, a convolutional layer preceding pooling and FC layers for classification decisions are implemented. FCN consists of three convolutional layers, with hidden dimension sizes sequentially set at 128, 256, and 256, and kernel sizes of 9, 5, and 3. ResNet comprises nine convolutional layers, with hidden dimension sizes sequentially set as 64×3 , 128×3 , 256×3 , and kernel sizes of $(9, 5, 3) \times 3$. SoM-TP is applied to the single pooling layer just before the FC layer in both model architectures. The FC layers of the CLS network and DPLN consist of three linear layers each. The FC layers of the CLS network are structured as follows: $256 * \text{number of segments} \times 512$, 512×1024 , $1024 \times \text{number of classes}$. On the other hand, the FC layers of the DPLN are structured as: $256 * \text{number of segments} * 3 \times 512$, 512×1024 , $1024 \times \text{number of classes}$.

Model Architecture Choice SoM-TP is a pooling method that fully leverages temporal information from the convolutional encoder. This implies that SoM-TP requires the utilization of the preserved information from the convolutional encoder. Consequently, an architecture capable of accumulating detailed information in deeper layers, such as ResNet, is suitable for SoM-TP. When SoM-TP replaces the final global average pooling layer in ResNet, it surpasses the performance of the vanilla ResNet.

Technically, SoM-TP can be implemented in intermediate pooling layers of models with multiple pooling stages. However, considering SoM-TP’s objective of selecting the optimal temporal pooling that fully reflects the formed representations, applying it to the accumulated information across all layers in the last layer is the most effective approach.

Detailed Training and Evaluation Procedures of SoM-TP The main distinction between training and evaluation is that the DPLN subnetwork is not used during evaluation. In the evaluation process, only the trained \mathbf{A}_0 and ϕ_0 are used to select the optimal pooling for each batch, leading to the generation of the output \mathbf{A} . Subsequently, the pooling output is selected from \mathbf{A} .

Network	#Conv.	# Segments		#FC.	Optim.	lr	batch	window	epoch
		GTP	STP&DTP						
FCN	3	1	n	3	Adam	$1e-4$	[1, 8]	1	300
ResNet	9	1	n	3	Adam	$1e-4$	[1, 8]	1	300
Data	Type			GTP	STP	DTP	λ decay		
UCR	FCN SoM-TP MAX			avg	avg	max	$1e-1$		
	ResNet SoM-TP MAX			avg	avg	max	$1e-1$		
UCR	FCN SoM-TP AVG			avg	avg	max	1.0		
	ResNet SoM-TP AVG			max	max	max	1.0		
UEA	FCN SoM-TP MAX			max	max	max	$1e-1$		
	ResNet SoM-TP MAX			max	max	avg	$1e-2$		
UEA	FCN SoM-TP AVG			max	max	max	$1e-1$		
	ResNet SoM-TP AVG			avg	max	max	$5e-3$		

Table 5: Optimal Hyper-parameters.

GTP		STP		DTP		FCN-UCR		FCN-UEA		Res-UCR		Res-UEA	
MAX	AVG	MAX	AVG	MAX	AVG	ACC	F1	ACC	F1	ACC	F1	ACC	F1
✓		✓		✓		0.7502	0.7195	0.6920	0.6621	0.7600	0.7319	0.6453	0.6187
					✓	0.7351	0.7062	0.6849	0.6554	0.7533	0.7214	0.6769	0.6387
				✓		0.7508	0.7223	0.6611	0.6439	0.7652	0.7382	0.6610	0.6300
					✓	0.7425	0.7125	0.6867	0.6590	0.7607	0.7318	0.6579	0.6325
✓		✓		✓		0.7515	0.7183	0.6644	0.6406	0.7628	0.7323	0.6598	0.6217
					✓	0.7370	0.6989	0.6707	0.6430	0.7713	0.7432	0.6516	0.6242
				✓		0.7556	0.7241	0.6848	0.6633	0.7773	0.7489	0.6734	0.6399
					✓	0.7398	0.7055	0.6539	0.6383	0.7678	0.7396	0.6573	0.6299

*This table is for SoM-TP pooling selection operation type MAX.

GTP		STP		DTP		FCN-UCR		FCN-UEA		Res-UCR		Res-UEA	
MAX	AVG	MAX	AVG	MAX	AVG	ACC	F1	ACC	F1	ACC	F1	ACC	F1
✓		✓		✓		0.7407	0.7147	0.6909	0.6753	0.7659	0.7389	0.6715	0.6523
					✓	0.7278	0.6984	0.6445	0.6169	0.7526	0.7239	0.6750	0.6270
				✓		0.7347	0.7084	0.6794	0.6412	0.7508	0.7200	0.6674	0.6249
					✓	0.7193	0.6894	0.6295	0.5982	0.7284	0.7012	0.6294	0.6050
✓		✓		✓		0.7469	0.7171	0.6295	0.6804	0.7476	0.7232	0.6764	0.6505
					✓	0.7136	0.6825	0.6563	0.6291	0.7303	0.7032	0.6467	0.6081
				✓		0.7562	0.7315	0.6800	0.6510	0.7437	0.7315	0.6722	0.6486
					✓	0.7198	0.6870	0.6531	0.6274	0.7373	0.7103	0.6602	0.6278

*This table is for SoM-TP pooling selection operation type AVG.

Table 6: Ablation Study on Pooling Operation in the Pooling Block. SoM-TP selects pooling by the MAX/AVG index of attention **A**, and this is referred to as SoM-TP’s operation. However, operations for each pooling within the pooling block can also vary. In other words, the ‘max’ and ‘avg’ operations of GTP, STP, and DTP can be hyperparameters in SoM-TP. We investigate the performance through ablation studies, and the best performance is indicated in bold.

Optimal Hyper-parameters The optimal hyperparameters for the results in Tables 1 and 2 can be found in Table 5. The batch size ranges from 1 to 8, with a default of 8 or one-tenth of the dataset size if the dataset size is under 80. The pooling operation occurs once in both the pooling block and DPL Attention **A**. In Table 5, ‘Type’ refers to the operation type (AVG, MAX) used when selecting pooling from DPL attention **A**. The operation (avg, max) for GTP, STP, and DTP denotes the pooling operation employed within the pooling block. The λ decay parameter represents the degree of influence of the perspective loss and is optimized within the range of [1e-5, 1.0]. The seed number is arbitrarily set to 10.

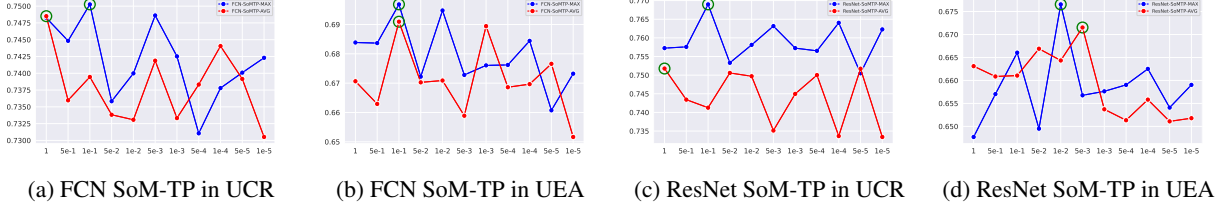


Figure 6: λ ablation study of SoM-TP. λ is the decay value of the perspective loss, a crucial hyperparameter in SoM-TP. Note that as λ increases, the perspective loss reflects all pooling perspectives more strongly. The ablation study covers λ values across the range of $[1, 1e-5]$ with 11 intervals. The blue and red lines correspond to the utilized pooling operation types, MAX and AVG, respectively. The optimal λ resulting in the highest performance is highlighted with a green circle.

How Does Perspective Loss Affect Pooling Ensemble? The degree of balanced pooling selection in SoM-TP is tunable by adjusting the similarity between the output distributions of f_{DPLN} and f_{CLS} using the perspective loss. The relationship between performance and the value of λ is depicted in Figure 6. Increasing λ facilitates the integration of multiple perspectives in the ensemble via the perspective loss. The optimal balance depends on the dataset and model characteristics. Nevertheless, when assessed across various UCR/UEA datasets, Table 3 indicates that the absence of perspective loss (without DPLN) considerably diminishes the effectiveness of the selection ensemble.

A Detailed Experiment on Batch SoM-TP selects the most proper pooling by minimizing the sum of losses for all samples within a batch. Therefore, we acknowledge that individual batches can have varying pooling selections based on their composition. However, since Attention \mathbf{A}_0 accumulates updates for each batch, it ultimately considers the entire dataset. Additionally, DPLN, through perspective loss, incorporates the results of other poolings not selected in the CLS network, making it robust to batch shuffling.

To confirm the robustness of SoM-TP to batch shuffling, we conduct experiments on 113 UCR datasets with FCN, using batch shuffling with 5 different seeds. The standard deviation of average performance for all datasets is 0.0046, affirming its robustness to batch variations.

Detailed Performance Analysis on SoM-TP

CNN	POOL (type)	UCR (uni-variate)					UEA (multi-variate)					
		ACC	F1 macro	ROC AUC	PR AUC	Rank	ACC	F1 macro	ROC AUC	PR AUC	Rank	
FCN	GTP	0.7227	0.6902	0.8838	0.7641	2.8	0.6642	0.6388	0.8067	0.6974	3.0	
	STP	<u>0.7302</u>	<u>0.6967</u>	0.8770	<u>0.7697</u>	<u>2.9</u>	<u>0.6816</u>	<u>0.6515</u>	0.8171	<u>0.7119</u>	2.6	
	DTP	euc	0.7137	0.6815	0.8735	0.7489	3.5	0.6449	0.6157	0.7722	0.6656	3.8
		cos	0.7106	0.6774	0.8701	0.7470	3.5	0.6372	0.6088	0.7780	0.6612	3.9
	SoM-TP	0.7562	0.7315	0.9016	0.7957	2.5	0.6909	0.6753	<u>0.8137</u>	0.7138	<u>2.7</u>	
ResNet	GTP	0.7544	0.7244	0.9137	0.8070	2.8	0.6419	0.6149	0.7845	0.6825	2.9	
	STP	<u>0.7583</u>	<u>0.7323</u>	0.8983	0.7996	2.6	<u>0.6612</u>	<u>0.6321</u>	<u>0.8022</u>	<u>0.6950</u>	<u>2.9</u>	
	DTP	euc	0.7258	0.6967	0.8797	0.7649	3.4	0.6475	0.6227	0.7886	0.6859	3.3
		cos	0.7256	0.6963	0.8735	0.7563	3.4	0.6299	0.6044	0.7672	0.6540	3.9
	SoM-TP	0.7659	0.7389	0.9038	<u>0.8026</u>	<u>2.7</u>	0.6764	0.6505	0.8081	0.7105	2.6	

*This table is for SoM-TP pooling selection operation type AVG.

Table 7: SoM-TP AVG Performance. Note that SoM-TP selects pooling by the MAX/AVG index of attention \mathbf{A} , referred to as SoM-TP’s operation. This table represents SoM-TP selection operation AVG performance compared to existing temporal poolings. The best performances are bolded, and the second-best performances are underlined.

Dynamic Selection of Temporal Poolings in SoM-TP

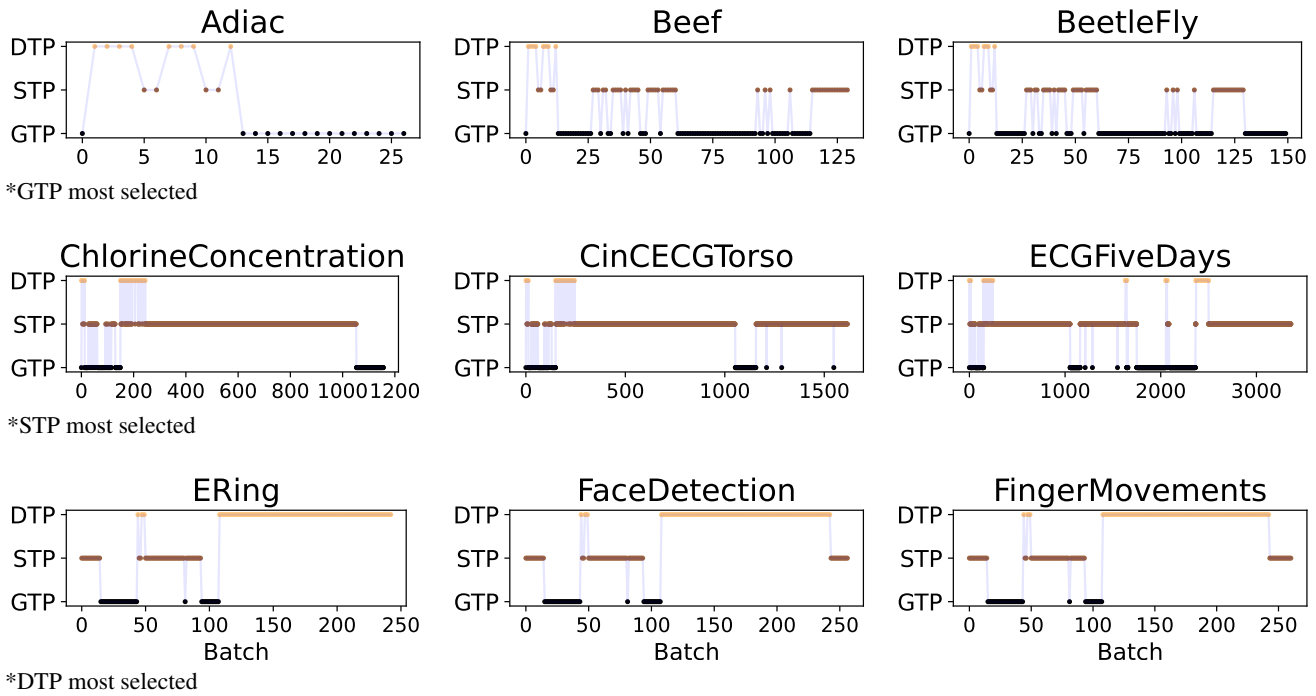


Figure 7: Dynamic Pooling Selection in SoM-TP. Expanding on Figure 3, this figure provides additional examples encompassing various time series data. Within this figure, we can examine the dynamic selection graph for FCN SoM-TP MAX on the UCR/UEA repository. We demonstrate that SoM-TP’s dynamic selection mechanism functions robustly across multiple datasets with diverse data sizes and time lengths during the inference process. Notably, samples labeled as ‘DTP most selected’ are chosen for datasets from the UEA repository, which typically present higher complexity compared to the UCR repository.

LRP Ablation Study on Different Temporal Poolings

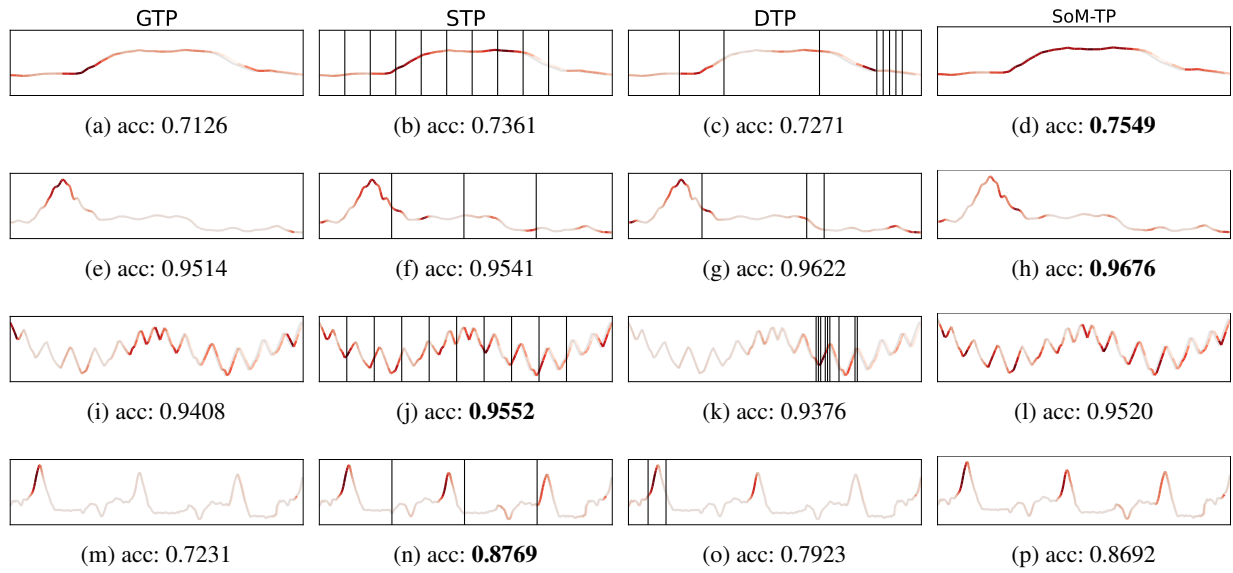


Figure 8: Comparing LRP Input Attribution: Fixed vs Diverse Perspective Learning. This figure represents the input attribution (LRP) of distinct temporal poolings on the UCR repository, specifically for the Crop, Strawberry, SwedishLeaf, and ToeSegmentation2 datasets. Following the row sequence, these instances correspond to two samples of SoM-TP’s best and STP’s best scenarios, respectively. The figure highlights that SoM-TP excels when learning from diverse perspectives. Even when it doesn’t rank as the best, the input attribution closely resembles that of the best independent pooling, ensuring robust performance.

Extended Experiment on Real-World Large Datasets

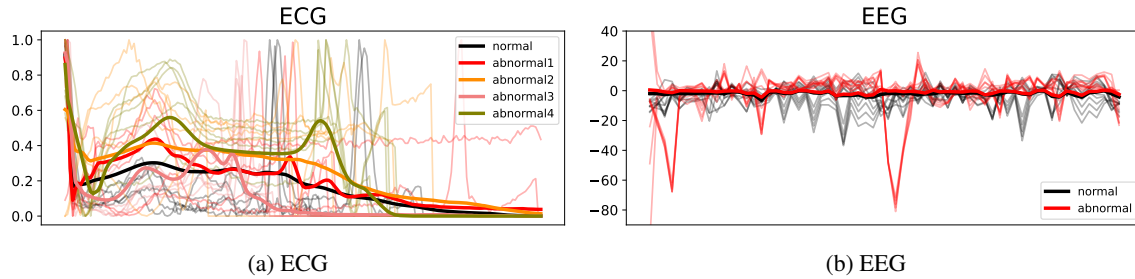


Figure 9: ECG and EEG Datasets. First, ECG is univariate time series data with 5 classes, as shown in (a), with the x-axis representing time and the y-axis representing values. Second, EEG is multivariate time series data with 2 classes, non-alcoholic vs. alcoholic, as shown in (b), with the x-axis representing 65 channels and the y-axis representing values.

Dataset	Type	#Size	#Class	#Conv.	#Pooled Prototypes	#FC.	Optim.	lr	batch	window	epoch
					GTP STP&DTP						
ECG	uni-variate	109,446	2	1	1	1	Adam	$1e-4$	256	1	100
EEG	multi-variate (65)	122,880	5	3	n	1	Adam	$1e-4$	256	10	100

Table 8: Detailed data description and experimental settings.

POOL (type)		ECG (uni-variate)				EEG (multi-variate)			
		ACC	F1 macro	ROC AUC	PR AUC	ACC	F1 macro	ROC AUC	PR AUC
GTP	MAX	0.9236	0.7384	0.9854	0.9034	<u>0.9323</u>	<u>0.9321</u>	0.9727	<u>0.9734</u>
	AVG	0.9371	0.7839	0.9914	<u>0.9347</u>	0.8821	0.8818	0.9426	0.9435
STP	MAX	0.9421	0.7866	<u>0.9918</u>	<u>0.9392</u>	0.9162	0.9160	0.9663	0.9645
	AVG	0.9340	0.7611	0.9908	0.9222	0.8866	0.8865	0.9533	0.9514
DTP	MAX-euc	0.8593	0.6991	0.9856	0.9022	0.9087	0.9084	0.9619	0.9630
	AVG-euc	<u>0.9508</u>	<u>0.8000</u>	0.9860	0.9063	0.9108	0.9105	0.9628	0.9628
	MAX-cos	0.9179	0.7308	0.9841	0.9027	0.9212	0.9209	0.9694	0.9663
SoM-TP	AVG-cos	0.8802	0.6979	0.9849	0.8883	0.8747	0.8736	0.9362	0.9389
	MAX	0.9566	0.8266	0.9923	0.9413	0.9510	0.9508	0.9829	0.9817
	AVG	0.9272	0.7765	0.9884	0.9129	0.9424	0.9421	0.9799	0.9810

Table 9: Model Performances. The best performance of SoM-TP is bolded, while the best performances of other temporal poolings are underlined.

Real-world Large Datasets in Time Series Classification: EEG and ECG The UCR/UEA repository contains an extensive collection of TSC datasets. However, the repository’s largest dataset size reaches only 30,000, which is relatively small. Thus, we further experiment on a large real-world dataset. Specifically, we choose the ECG dataset (Kachuee, Fazeli, and Sarrafzadeh 2018) and the EEG dataset (Bay et al. 2000), both of which are highly representative in the medical field. ECG pertains to univariate and multi-class classification, while EEG involves multivariate and binary classification tasks. These datasets comprise more than 100,000 data points each, and in the case of the multivariate dataset, the number of feature columns is 65. Therefore, this experiment encompasses datasets that are not covered by the existing benchmark repository.

Experimental Settings First, for the ECG dataset, optimal results are achieved by adopting a shallow model with only one convolutional layer, as opposed to a deep model with multiple layers. Conversely, the EEG dataset demonstrates superior performance with FCN utilizing three convolutional layers. Regarding the batch size, a uniform setting of 256 is applied, taking into consideration the dataset size. For the EEG dataset, a window size of 10 is employed, meaning the previous 10 time steps serve as input for the model.

Performance Analysis SoM-TP MAX demonstrates outstanding performance across both the EEG and ECG datasets. Notably, we extend the evaluation beyond accuracy, utilizing F1-score, ROC-AUC, and PR-AUC to address class imbalance issues. Remarkably, SoM-TP consistently outperforms existing temporal pooling methods in all of these evaluation metrics. Moreover, the experiment reveals that DTP is not always dominant over GTP or STP. Nevertheless, SoM-TP exhibits robust performance regardless of dataset conditions.

DTP Algorithm

DTP is a pooling layer optimized by soft-DTW for dynamic segmentation considering the temporal relationship. The DTW distance is calculated through point-to-point matching with temporal consistency,

$$\text{DTW}_\gamma(X, Y) = \min_\gamma \{ \langle A, \Delta(X, Y) \rangle, \forall A \in \mathcal{A} \},$$

$$\min_\gamma \{ a_1, \dots, a_n \} = \begin{cases} \min_{i \leq n} a_i, & \gamma = 0 \\ -\gamma \log \sum_{i=1}^n e^{-a_i/\gamma}, & \gamma > 0, \end{cases} \quad (9)$$

where \mathbf{X} and \mathbf{Y} are time series with lengths t_1 and t_2 , and the cost matrix $\Delta(\mathbf{X}, \mathbf{Y}) \in \mathbb{R}^{t_1 \times t_2}$ represents the distance between \mathbf{X}_{t_1} and \mathbf{Y}_{t_2} . DTW is defined as the minimum inner product of the cost matrix with any binary alignment matrix $\mathcal{A} \in 0, 1^{t_1 \times t_2}$ (Lee, Lee, and Yu 2021; Cuturi and Blondel 2017). With the soft-DTW algorithm, similar time sequences are grouped with different lengths.

Algorithm 2: Dynamic Temporal Pooling

Function DTP (\mathbf{P}, \mathbf{H}):

$$\delta(p_l, h_t) = 1 - \frac{p_l \cdot h_t}{\|p_l\|_2 \|h_t\|_2}$$

Function forward (\mathbf{P}, \mathbf{H}):

- ▷ fill the alignment cost matrix $R \in \mathbb{R}^{L \times T}$
- $R_{0,0} = 0, R_{:,0} = R_{0,:} = \infty$
- for** $l = 1, \dots, L$ **do**
- for** $t = 1, \dots, T$ **do**
- $R_{l,t} = \delta(p_l, h_t) + \min_\gamma \{ R_{l-1,t-1}, R_{l,t-1} \}$
- return** $\text{DTW}_\gamma(\mathbf{P}, \mathbf{H}) = R_{L,T}$

Function backward (\mathbf{P}, \mathbf{H}):

- ▷ fill the soft alignment matrix $E \in \mathbb{R}^{L \times T}$
- $E_{l,t} = \partial R_{L,T} / \partial R_{l,t}$
- $E_{:,T+1} = E_{L+1,:} = 0$
- $R_{:,T+1} = R_{L+1,:} = -\infty$
- for** $l = L, \dots, 1$ **do**
- for** $t = T, \dots, 1$ **do**
- $a = \exp \frac{1}{\gamma} (R_{l,t+1} - R_{l,t} - \delta(p_l, h_{t+1}))$
- $b = \exp \frac{1}{\gamma} (R_{l+1,t+1} - R_{l,t} - \delta(p_{l+1}, h_{t+1}))$
- $E_{l,t} = a \cdot E_{l,t+1} + b \cdot E_{l+1,t+1}$
- return** $\nabla_P \text{DTW}_\gamma(\mathbf{P}, \mathbf{H}) = (\frac{\partial \Delta(\mathbf{P}, \mathbf{H})}{\partial \mathbf{P}})^T E$

Function optimization ($(\mathbf{X}, y), \mathbf{P}, \Phi$):

- ▷ \mathcal{W} : network Φ parameter
- ▷ $w^{(c)} \in \mathbb{R}^K$ of class weight vector
- ▷ $\mathbf{W}^c = [w_1^{(c)}, \dots, w_L^{(c)}] \in \mathbb{R}^{k \times L}$ of class weight matrix
- ▷ $P(y = c | \mathbf{X}) = \frac{\exp(\sum_{l=1}^L \bar{h}_l \cdot w_l^{(c)})}{\sum_{c'=1}^L \exp(\sum_{l=1}^L \bar{h}_l \cdot w_{l'}^{(c)})}$ of posterior
- $\mathcal{L}_{proto}(\mathbf{P}) = \frac{1}{N} \sum_N \text{DTW}_\gamma(P, \Phi(\mathbf{X}^n; \mathcal{W}))$
- $\mathcal{L}_{class}(\mathcal{W}, \{\mathbf{W}^{(c)}\})$
- $= -\frac{1}{N} \sum_{n=1}^N \log P(y = y^n | \mathbf{X}^n)$

Function optimize ($\mathbf{P}, \mathbf{W}, \mathcal{W}$):

- $\mathbf{P} \leftarrow \mathbf{P} - \eta \cdot \partial \mathcal{L}_{proto} / \partial \mathbf{P}$
- $\mathcal{W} \leftarrow \mathcal{W} - \eta \cdot \mathcal{L}_{class} / \partial \mathcal{W}$
- $\mathbf{W}^{(c)} \leftarrow \mathbf{W}^{(c)} - \eta \cdot \partial \mathcal{L}_{class} / \partial \mathbf{W}^{(c)}$
